DNA Repair 24 (2014) 113–121

Contents lists available at ScienceDirect

DNA Repair

journal homepage: www.elsevier.com/locate/dnarepair

In vivo evidence that DNA polymerase kappa is responsible for error-free bypass across DNA cross-links induced by mitomycin C

Akira Takeiri[a,*,1], Naoko A. Wada[a,1], Shigeki Motoyama[a], Kaori Matsuzaki[a], Hiromi Tateishi[b], Kaoru Matsumoto[b], Naoko Niimi[c,2], Akira Sassa[c], Petr Grúz[c], Kenichi Masumura[c], Masami Yamada[c], Masayuki Mishima[a], Kou-ichi Jishage[a], Takehiko Nohmi[c,**]

[a] *Research Division, Chugai Pharmaceutical Co., Ltd., 1-135 Komakado, Gotemba, Shizuoka 412-8513, Japan*
[b] *Gotemba Branch, Chugai Research Institute for Medical Science, Inc., 1-135 Komakado, Gotemba, Shizuoka 412-8513, Japan*
[c] *Division of Genetics and Mutagenesis, National Institute of Health Sciences, 1-18-1 Kamiyoga, Setagaya, Tokyo 158-8501, Japan*

ARTICLE INFO

Article history:
Received 12 June 2014
Received in revised form 4 August 2014
Accepted 10 September 2014
Available online 7 October 2014

Keywords:
DNA polymerase kappa
Knock-in mice
Gpt delta mice
Cross-links
Mitomycin C

ABSTRACT

Translesion DNA synthesis (TLS) is an important pathway that avoids genotoxicity induced by endogenous and exogenous agents. DNA polymerase kappa (Polk) is a specialized DNA polymerase involved in TLS but its protective roles against DNA damage *in vivo* are still unclear. To better understand these roles, we have established knock-in mice that express catalytically-inactive Polk and crossbred them with *gpt* delta mice, which possess reporter genes for mutations. The resulting mice (inactivated Polk KI mice) were exposed to mitomycin C (MMC), and the frequency of point mutations, micronucleus formation in peripheral erythrocytes, and γH2AX induction in the bone marrow was determined. The inactivated Polk KI mice exhibited significantly higher frequency of mutations at CpG and GpG sites, micronucleated cells, and γH2AX foci-positive cells than did the Polk wild-type (Polk$^+$) mice. Recovery from MMC-induced DNA damage, which was evaluated by γH2AX induction, was retarded in embryonic fibroblasts from the knock-in mice when compared to those from the Polk$^+$ mice. These results suggest that Polk mediates TLS, which suppresses point mutations and DNA double-strand breaks caused by intra- and interstrand cross-links induced by MMC treatment. The established knock-in mice are extremely useful to elucidate the *in vivo* roles of the catalytic activity of Polk in suppressing DNA damage that was induced by a variety of genotoxic stresses.

1. Introduction

The human genome is continuously exposed to a variety of endogenous and exogenous genotoxic insults, e.g. by reactive oxygen species and alkylating agents from endogenous sources, and by cigarette smoke, aflatoxins, and chemotherapeutic agents from exogenous sources [1]. These agents induce DNA damage in the form of DNA adducts, abasic sites, DNA strand cross-links, and single- and double-stranded breaks in DNA [2,3]. Such lesions are repaired by a number of mechanisms within the cell but, because chromosomal replication occurs before all lesions are removed, DNA polymerases (Pols) involved in replication will inevitably encounter the lesions. One strategy that cells develop to deal with the lesions is translesion DNA synthesis (TLS), in which the replication fork directly passes over DNA damage by means of specialized Pols [4–6]. Unlike Pols responsible for chromosomal replication, which stall at or before the lesions [7,8], the specialized Pols can bypass DNA lesions and continue primer extension beyond them [9]. It is assumed that the replicative Pols would take over the primer from the specialized Pols after successful TLS, thereby accomplishing the whole chromosomal replication [10].

* Corresponding author at: Fuji-Gotemba Research Laboratories, Chugai Pharmaceutical Co., Ltd., 1-135 Komakado, Gotemba, Shizuoka 412-8513, Japan. Tel.: +81 550 87 9342; fax: +81 550 87 6383.
** Corresponding author. Present address: Biological Safety Research Center, National Institute of Health Sciences, 1-18-1 Kamiyoga, Setagaya, Tokyo 158-8501, Japan. Tel.: +81 3 3700 1564; fax: +81 3 3700 1622.
E-mail addresses: takeiriakr@chugai-pharm.co.jp (A. Takeiri), nohmi@nihs.go.jp (T. Nohmi).
[1] Both the authors contributed equally to this work.
[2] Present address: Department of Sensory and Motor Systems, Tokyo Metropolitan Institute of Medical Science, 2-1-6 Kamikitazawa, Setagaya, Tokyo 156-8506, Japan.

http://dx.doi.org/10.1016/j.dnarep.2014.09.002
1568-7864/

Pol kappa (Polk) is a specialized Pol that belongs to the Y family, the most abundant class of Pols involved in TLS [11–14]. Polk is unique in that its orthologs are present in Eukarya, bacteria and Archaea [15–17]. Several lines of *in vitro* evidence suggest that Polk may be involved in TLS across a variety of DNA damage, such as N^2-guanyl adducts induced by polycyclic aromatic hydrocarbons and alkylating agents [18–23], a C8-guanyl adduct by 2-amino-1-methyl-6-phenylimidazo[4,5-*b*]pyridine (PhIP) [24], thymine glycol [25,26], 8-oxo-guanine [27,28], and interstrand DNA cross-links [29]. In addition to TLS, Polk is reported to be involved in nucleotide excision repair [30], replication checkpoint [31], repair of single-strand breaks in DNA [32], and microsatellite stability [33]. Knockout (KO) mice of Polk are viable and exhibit more frequent spontaneous mutations in liver, lung, and kidney in aged mice [34,35]. However, it is still unclear which of the DNA lesions Polk protects cells from *in vivo* (the whole body system) and what roles it plays in preventing cancer induced by environmental stresses.

To understand better the *in vivo* protective roles, we have established knock-in (KI) mice where inactive Polk is expressed from its cognate promoter. Two essential amino acids for Pol activity, Asp197 and Glu198, were changed to Ala and Ala in the KI mice (*Polk*$^{D197A-E198A}$ mice). We generated KI mice instead of KO mice because Polk interacts with other proteins, such as REV1 and PCNA [23,36–38]. REV1 interacts with Pol eta, Pol iota, and REV3L (a catalytic subunit of Pol zeta) [39], and PCNA interacts with a number of proteins involved in DNA transactions [40]. Therefore, a simple KO or knockdown of Polk might possibly modulate the functions of other proteins, thereby obscuring the intrinsic roles of Polk, which depend on a catalytic activity as a DNA polymerase and on protein–protein cross-talks with other DNA replication components to maintain the genome stability. We crossed the *Polk*$^{D197A-E198A}$ mice with *gpt* delta mice [41], which possess reporter genes for mutations *in vivo*. The *gpt* delta mice have been extensively employed in chemical mutagenesis, carcinogenesis, and radiation biology [42–44]. We exposed the resulting mice, namely, inactivated Polk mutant and *gpt* delta double transgenic mice (hereafter, referred to as inactivated Polk KI mice, and their counterparts, the Polk wild-type *gpt* delta mice, as Polk$^+$ mice) to mitomycin C (MMC). Then gene mutations and DNA damage induced by MMC in these mice were evaluated in bone marrow, which is widely known as a target tissue of MMC. We chose MMC as the first genotoxic agent to be assayed on inactivated Polk KI mice because the chemotherapeutic agent induces interstrand and intrastrand cross-links in DNA [45]. Interstrand cross-links prevent strand separation of DNA, which inhibits DNA replication, transcription, and translation. Although several Pols such as Pol zeta, Rev1, and Polk are suggested to be involved in TLS across lesions that have been unhooked from the cross-linked DNA during repair [46], *in vivo* evidence of which Pols participate in the repair process is missing. In addition, the Pols responsible for TLS across intrastrand cross-links, which are much more abundant after MMC treatment than the interstrand cross-links, have been less thoroughly investigated [47]. The results from inactivated Polk KI mice suggest that Polk plays significant roles in protecting cells against genotoxicity of the inter- and intrastrand

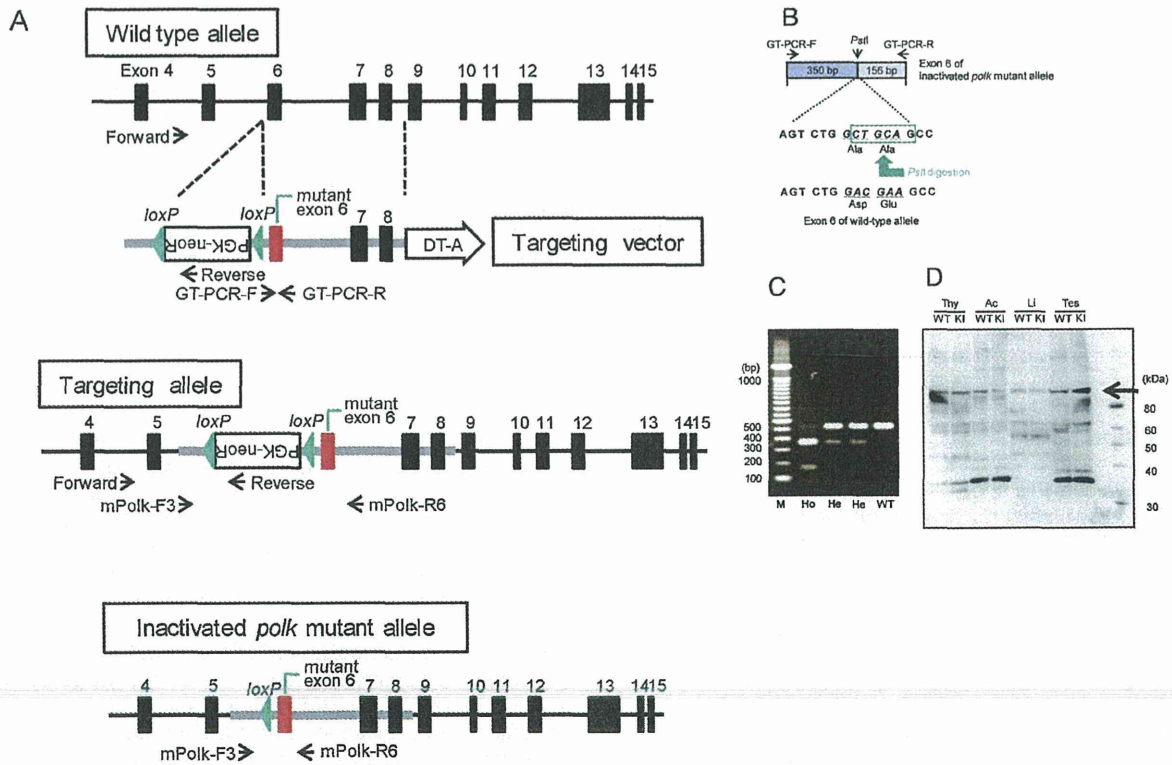

Fig. 1. Generation of inactivated Polk KI mice. (A) Structure of a targeting vector for inactivation of mouse *Polk*, and the predicted structures of the targeted and inactivated *Polk* mutant alleles. The latter allele was generated from the former by Cre-loxP mediated recombination. PCR primers for genotyping are shown by horizontal arrows. (B) The exon 6 of inactivated Polk KI mice. Wild type codons GAC GAA were substituted to GCT GCA in inactivated Polk KI mice to introduce the *Pst*I digestion site. (C) An agarose gel electrophoresis image for PCR products of mouse Polk exon 6 after *Pst*I digestion. Polk wild-type (WT) allele is insusceptible to *Pst*I digestion. A PCR product from homo genotype of *Polk* mutant (Ho) shows two fragments digested by *Pst*I. Hetero genotype of *Polk* mutant (He) shows both the wild-type allele band and the *Pst*I fragments. (D) Western blotting analyses of the wild-type Polk expressed in wild-type mice (WT) and the Polk derivative with D197A-E198A in *Polk*$^{D197A-E198A}$ mice (KI). Cell extracts (20 μg) of thymus (Thy), adrenal cortex (Ac), liver (Li), and testis (Tes) from the mice were applied to each lane. The arrow indicates the position of Polk and Polk derivative with D197A-E198A.

cross-links by carrying out error-free TLS. Modulation of Polk activity may be important for suppressing secondary tumors associated with MMC treatment. The contribution of other Pols in TLS during repair against cross-links is also discussed.

2. Materials and methods

2.1. Animals

2.1.1. Generation of Polk$^{D197A-E198A}$ Mice

All animal care and experiment procedure in this study were conducted in compliance with the internal regulations for animal use at Chugai Pharmaceutical Co., Ltd., which have been approved by the Association for Assessment and Accreditation of Laboratory Animal Care International.

The targeting vector for *Polk*$^{D197A-E198A}$ mice, which had mutations directing the expression of D197A-E198A, was designed (Fig. 1A). Briefly, to change the amino acids, the endogenous sequence (5′-AGT CTG GAC GAA GCC-3′) in exon 6 of mouse *Polk* was changed to a mutant sequence (5′-AGT CTG GCT GCA GCC-3′). A fragment of the neomycin resistance (*neo*) gene flanked by two *loxP* sequences was inserted into intron 5. C57BL/6N embryonic stem (ES) cells transfected with the linearized targeting vector were cultured in a medium supplemented with G418 for 10 days. Homologous recombinant ES cell clones were screened for inactivated *Polk* mutants by PCR using a primer pair of Forward (5′-ATCGATATGTCCATTTAGGGATGTT-3′) and Reverse (5′-CTTCCTCGTGCTTTACGGTATC-3′) to amplify the exon 5 region including a target vector fragment (Fig. 1A). PCR products of the *Polk* mutants were detected at 3.29 kbp. The *Polk* mutant allele was confirmed by *Pst*I digestion pattern of PCR products amplified with a primer set of GT-PCR-F (5′-CTTTCTGTTCCTACCAGAATAATGC-3′) and GT-PCR-R (5′-TATATTCCAAGAGCTGCTTTCTGTT-3′) (Fig. 1B and C). The mutations were confirmed by DNA sequencing analyses. The *Polk* mutant ES cell clones were injected into BALB/cA blastocysts to produce chimera mice. The chimera mice were bred with C57BL/6N females to generate offspring with the *Polk* mutant allele. After confirmation of germline transmission, the floxed *neo* gene cassette was removed from the *Polk* mutant allele by pronuclear microinjection of the Cre recombinase expression vector, pMacII-Cre [48]. Removal of the *neo* gene cassette was confirmed by PCR using a primer pair mPolk-F3 (5′-CAGGATGTCACGTTCATTAA-3′) and mPolk-R6 (5′-CCAAGAGCTGCTTTCTGTT-3′). PCR products of the *Polk* mutant allele with and without the *neo* cassette were detected at 3.26 kbp and 1.26 kbp, respectively. After homogenization of the *Polk* mutant allele, C57BL6-*Polk*$^{tm3(mPolk)Csk}$ mice, referred to in this study as *Polk*$^{D197A-E198A}$ mice, were established. The Western blotting for the expression of D197A-E198A and wild-type Polk in *Polk*$^{D197A-E198A}$ mice and littermate wild-type mice, respectively, was conducted with polyclonal antisera against human Polk [21].

2.1.2. Generation of Inactivated Polk KI Mice

The *gpt* delta mice, which have lambda EG10 DNA as a reporter for mutations, were previously reported [41,42]. The *Polk*$^{D197A-E198A}$ mice were bred with *gpt* delta mice, and then the successful double transgenic mice were selected by PCR using a primer pair GT-PCR-F and GT-PCR-R for the *Polk* mutations and SYYA0602-1 (5′-GCGCAACCTATTTTCCCCTCGA-3′) and SYYA0602-2 (5′-TGGAAACTATTGTAACCCGCCTG-3′) for the *gpt* delta transgene. The offspring (*Polk* mut/–, lambda EG10 Tg/Tg) were intercrossed to produce double homozygous (*Polk* mut/mut, lambda EG10 Tg/Tg) mice. Consequently, the inactivated Polk KI mice, that is to say, the *Polk* mut/mut, lambda EG10 Tg/– or *Polk* mut/mut, lambda EG10 Tg/Tg, were established. The formal name of the inactivated Polk KI mice is C57BL6-*Polk*$^{tm3(mPolk)Csk}$ *Tg(gptdelta)1Nmi*.

2.2. MMC treatment and sample collection

For mutation analyses, the inactivated Polk KI mice (*Polk* mut/mut, lambda EG10 Tg/–) and Polk^{+} mice (*Polk* wt/wt, lambda EG10 Tg/–) were treated with MMC (CAS No. 50-07-7, Kyowa Hakko Kogyo, Tokyo, Japan) intraperitoneally at a dose of 1 mg/kg/day for 5 consecutive days (Fig. S1). Saline served as a solvent control. Six 13–14-week-old female inactivated Polk KI mice were used for each MMC- and saline-treated group. Four 12–13-week-old female Polk^{+} mice were used for each treatment group. Bone marrow cells were collected from femurs one week after the final administration. For the 1st micronucleus (MN) assay, small aliquots of peripheral blood were collected from the dorsal metatarsal veins of the hind foot of Polk^{+} and inactivated Polk KI mice before each injection of MMC during the five consecutive treatments. For the 2nd MN assay and γH2AX evaluation, the inactivated Polk KI mice (*Polk* mut/mut, lambda EG10 Tg/Tg) and Polk^{+} mice (*Polk* wt/wt, lambda EG10 Tg/Tg) were treated with MMC in the same manner as described above. Three male and 3 female 10–12-week-old mice of each genotype were used for each MMC- and saline-treated group. For MN detection, small aliquots of peripheral blood were collected 24 h after the second injection of MMC during the five consecutive treatments. For γH2AX evaluation, bone marrow cells were collected from the femurs 3 h after the final administration.

2.3. Mutation frequency (MF) and mutation spectrum analyses

MF in bone marrow was measured by 6-thioguanine (6-TG) selection and Spi^{-} selection according to the previous report [42]. At least 1×10^6 colonies or phage plaques were recovered from genomic DNA of each animal. DNA sequences of the *gpt* genes in 6-TG resistant mutants, and those of the *gam* gene and the flanking region in Spi^{-} mutants were determined by DNA sequence analysis. Each mutation was classified to determine the mutation spectra. Identical mutations obtained from the same mouse were regarded as clonally propagated mutants and counted as one mutation and the MF was compensated. Specific MF was calculated by multiplying the group MF by the ratio of the number of mutations for each type of mutation. Statistics analyses were conducted according to the method of Carr and Gorelick [49].

2.4. MN assay

The peripheral blood samples were smeared on slide glass and fixed with methanol. Micronucleated erythrocytes among 2000 immature erythrocytes stained with acridine orange were microscopically counted for each mouse. The ratios of immature erythrocytes in total 1000 erythrocytes were determined.

2.5. Measurement of bone marrow cells with γH2AX foci

The bone marrow cells were fixed with 4% paraformaldehyde in phosphate buffered saline (PBS). The cells were rinsed with 5% (v/v) heat-inactivated fetal bovine serum (FBS) in PBS and resuspended in PBS. Cold ethanol was added to the suspension to be approximately 70% and stored at −20 °C. The cells resuspended in PBS were stained with anti-γH2AX (Ser139) antibody (Abcam, Cambridge, UK) and Alexa Fluor 488 conjugated goat anti-mouse IgG antibody (Invitrogen). The cells on cytospin-prepared slides were embedded into antifade reagent (Invitrogen) including 4′,6-diamidino-2-phenylindole (DAPI). Cells with γH2AX foci out of more than 1200 cells in each mouse were counted. Image capture and analysis was conducted using InCell Analyzer 6000 and imaging software (GE healthcare Japan, Tokyo, Japan).

2.6. Measurement of γH2AX in mouse embryonic fibroblasts (MEFs)

MEFs were prepared from 13.5 days postcoitum embryos of inactivated Polk KI mice (*Polk* mut/mut, lambda EG10 Tg/Tg) and Polk$^+$ mice (*Polk* wt/wt, lambda EG10 Tg/Tg). Cells were cultured in Dulbecco's modified Eagle's medium (Sigma–Aldrich, St. Louis, MO, USA) supplemented with 10% FBS in a humidified atmosphere of 5% CO_2 at 37 °C. Each MEF seeded in 96-well plates at 5×10^3 cells/well. One day after the seeding, the cells were treated with MMC at doses of 2–1000 ng/mL for 24 h. The cells were fixed with methanol 24, 72, and 120 h after the commencement of treatment. Cells were stained with anti-γH2AX (Ser139) antibody (Millipore, Billerica, MA, USA) and Alexa Fluor 488 conjugated goat anti-mouse IgG antibody (Invitrogen). Fluorescence intensity of γH2AX per nucleus out of more than 200 cells was measured. The nuclei and cytoplasm were stained with Hoechst 33258 and CellMaskRed (Invitrogen), respectively. Image capture and analysis were conducted using ArrayScan HCS Reader and imaging software (Thermo Fisher Scientific, Waltham, MA, USA).

3. Results

3.1. Generation of inactivated Polk KI mice

The targeting vector used to make inactivated Polk KI mice was designed to change the amino acids that are critical for Polk catalytic activity, Asp197 and Glu198, to two alanine (Fig. 1A, B). C57BL/6N ES cells were transfected with a linearized targeting vector by electroporation, and homologous recombinant ES cell clones were screened by PCR. The PCR products of the *Polk* mutant allele were detected at 350 bp and 156 bp and those of the wild allele were detected at 506 bp after *Pst*I digestion (Fig. 1C). The *Polk* mutant allele was confirmed by DNA sequence analysis. In total, 8 clones of homologous recombinant ES cell clones were injected into blastocysts to generate the chimera mice. The chimeras of 7 clones were bred with C57BL/6N mice to produce heterozygote mice. We obtained three independent mutant mouse lines, which had floxed *neo* sequences. To remove the *neo* gene cassette, pMacII-Cre was injected into fertilized eggs of lines #1H1 and #2G1 of *Polk* mutant heterozygotes. After homogenization of the *Polk* mutant allele, two lines of double transgenic mice were established independently by breeding with *gpt* delta mice. Both lines had identical mutations directing Asp197-Glu198 to Ala-Ala of Polk (D197A-E198A) in both chromosomes and possessed lambda EG10 DNA, which carries the reporter genes for *in vivo* mutations, *gpt* and *red/gam* [41]. We used line #1H1 *gpt* delta mice for further examinations. To determine whether the Polk derivative harboring D197A-E198A is expressed at levels comparable to that of the wild-type Polk, we conducted Western blotting analyses. Bands corresponding to the expected molecular size of mouse Polk (96 kDa) were detected and the band pattern of proteins was similar to that in a previous report [50]. The similar intensity in the thymus, adrenal cortex, liver, and testis were detected between the targeted and the wild-type mice (Fig. 1D). In separate experiments, we confirmed that the derivative of Polk that has D197A-E198A lost Pol catalytic activity *in vitro* (Figs. S2 and S3).

3.2. MMC-induced mutations at CpG or GpG sites in bone marrow of mice

We treated inactivated Polk KI mice and Polk$^+$ mice with MMC, and analyzed mutations in the bone marrow by two mutation selection systems, 6-TG and Spi$^-$ selections. Firstly, in the 6-TG selection, which predominantly detects base substitutions in the *gpt* gene [42], MF of the tandem base substitutions at GpG sites, such as 5′-GG-3′ to 5′-TA-3′, was significantly enhanced by MMC treatment in inactivated Polk KI mice (9.6×10^{-7} versus 0, $p < 0.01$, Fig. 2A, Table S1), while no significant induction was observed in the Polk$^+$ mice (2.8×10^{-7} versus 0). Although the difference was not statistically significant, MF in inactivated Polk KI mice was about three times higher than in Polk$^+$ mice (9.6×10^{-7} versus 2.8×10^{-7}). In addition, MF of G:C to T:A transversions was significantly enhanced by MMC treatment in inactivated Polk KI mice (17.6×10^{-7} versus 6.0×10^{-7}, $p < 0.05$), whereas no significant induction was observed in Polk$^+$ mice (11.3×10^{-7} versus 4.0×10^{-7}). The tandem base substitutions and the transversions in inactivated Polk KI mice were mainly identified at three sites: 5′-C<u>C</u>G-3′, 5′-CC<u>G</u>-3′, and 5′-C<u>GG</u>-3′ (Fig. S4), with the underlined bases being changed.

The second selection, Spi$^-$, detects frameshifts and base substitutions in the *gam* gene and large deletions in the *red/gam* genes [42,51]. In the selection, MF of single-base deletions at monotonous G or C run sequences, such as 5′-GGGG-3′ to 5′-GGG-3′, in the *gam* gene was enhanced by MMC treatment significantly in inactivated Polk KI mice (17.7×10^{-7} versus 9.8×10^{-7}, $p < 0.05$, Fig. 2B, Table S2). In contrast, no significant increase was observed in the MF in MMC-treated Polk$^+$ mice (5.1×10^{-7} versus 4.8×10^{-7}). In addition, MF of single- and tandem-base substitutions, insertions and short sequence substitutions at 5′-CpG-3′ or 5′-GpG-3′ sequence, such as 5′-CG-3′ to 5′-AA-3′, was enhanced by MMC treatment significantly in Polk KI mice (19.6×10^{-7} versus 2.4×10^{-7}, $p < 0.01$, Fig. 2B, Table 1, S2). No significant increase was observed in the MF of MMC-treated Polk$^+$ mice (3.4×10^{-7} versus 1.6×10^{-7}). The frequency of these mutations induced by MMC was about six times higher in inactivated Polk KI mice than in Polk$^+$ mice, and the difference was statistically significant (19.6×10^{-7} versus 3.4×10^{-7}, $p < 0.01$). Besides single deletions and substitutions, several large deletions mostly with a size of more than 1 kb were detected (Table S3 and Fig. S5). However, the MF of such deletions was not obviously different between MMC- and saline-treated groups in either inactivated Polk KI or Polk$^+$ mice.

Table 1
Sequence changes at CpG, GpG or their neighboring sites in the *gam* gene of Spi$^-$ mutants recovered from MMC-treated or saline-treated groups of Polk$^+$ and inactivated Polk KI mice.

Mice	Treatment	Animal ID	Position in the *gam* gene	Sequence change[a]
Polk$^+$	Saline	103	212	acTgg → acCgg
	MMC	202	140–142	cAGGat → cTTatc
		202	314	tgCgt → tgAgt
		202	189–192	gcCCgTga → gcAAgAAga
		204	236	*cc*Tgc → ccCgc
Inactivated Polk KI	Saline	305	177	taCca → taAca
		305	236	*cc*Tgc → ccAgc
	MMC	401	286–289	acggggcc → acggggGcc
		402	177–178	taCCag → taAAag
		402	127	*ac*Gct → acCAct
		402	257–258	atCGct → atAAct
		403	286–289	acggggcc → acggggGcc
		403	314	tgCgt → tgAgt
		404	344	gcGca → gcCca
		404	314	tgCgt → tgAgt
		405	177–178	taCCag → taATag
		406	177	taCca → taAca

[a] Substituted bases are noted with capitals, and CpG and GpG sites are italicized.

3.3. MMC-induced MN in bone marrow of mice

Next, we tested the protective role of Polk against clastogenicity of MMC in an MN assay in bone marrow. The percentage of MN in peripheral immature erythrocytes was elevated concomitantly with consecutive treatments of MMC in both inactivated Polk KI and Polk$^+$ mice (Table S4). Interestingly, the percentage of MN

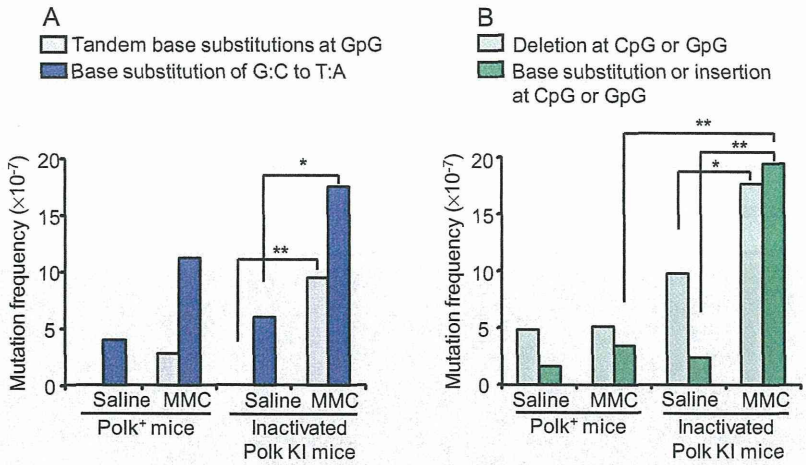

Fig. 2. MFs in 6-TG selection (A) and Spi⁻ selection (B) in the bone marrow. Bone marrow cells were obtained 1 week after the 5-day consecutive intraperitoneal treatments with saline or MMC at 1 mg/kg/day from inactivated Polk KI and Polk⁺ mice. (A) MF of tandem-base substitutions at GpG sites, e.g., 5′-GG-3′ to 5′-TA-3′, and single-base substitutions of G:C to T:A. (B) MF of single-base deletions, e.g., 5′-GGGG-3′ to 5′-GGG-3′, and base substitutions in the *gam* gene at CpG, GpG or their flanking sequences, e.g., 5′-GG-3′ to 5′-TT-3′. * and ** means $p < 0.05$ and $p < 0.01$ by Fisher's exact test, respectively. For the details, see Tables S1 and S2.

incidence in inactivated Polk KI mice was slightly but significantly higher than that of Polk⁺ mice at day two (5.2 ± 0.5 versus 3.7 ± 1.8, $p < 0.05$). The frequency of MN incidence was similar between the two types of mice at day 4 (7.3 ± 2.3 versus 6.2 ± 2.8). To confirm the initial results, we conducted a second MN assay focusing on the percentage of MN incidence at day 2 (Fig. 3). The percentage of MN incidence in inactivated Polk KI mice was significantly higher than that of Polk⁺ mice (6.5 ± 2.2 versus 4.3 ± 0.7, $p < 0.05$), which was very similar to the initial results. The ratio of immature erythrocytes in total erythrocytes, which is a marker of erythropoiesis, was decreased by MMC administration, but there was no significant difference between inactivated Polk KI and Polk⁺ mice. Therefore, we concluded that the higher percentage of MN incidence in inactivated Polk KI than Polk⁺ mice was due to the inefficiency of inactivated Polk KI mice to suppress double-strand breaks in DNA (DSBs) induced by MMC compared to Polk⁺ mice.

3.4. Bone marrow cells with γH2AX foci in MMC-treated mice

To further examine the roles of Polk to protect cells from DSBs by MMC, bone marrow cells having γH2AX foci (γH2AX positive cells) were counted at day 4 (Fig. S1). The number of the γH2AX positive cells was elevated by treatments of MMC in both inactivated Polk KI and Polk⁺ mice (Fig. 4). The incidence of γH2AX positive cells in inactivated Polk KI mice was slightly but significantly higher than in Polk⁺ mice (80% versus 75%, $p < 0.05$).

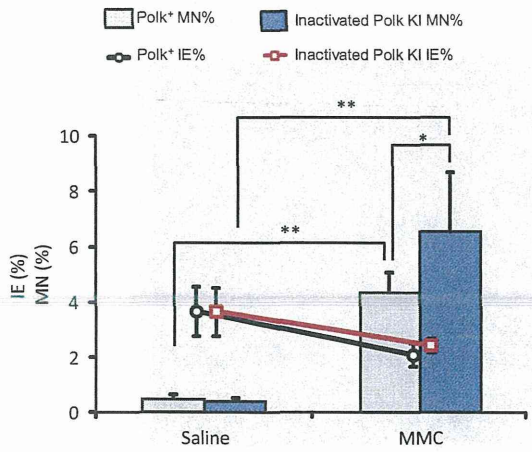

Fig. 3. MN induction by MMC treatment in Polk⁺ and inactivated Polk KI mice. Incidence of micronucleated peripheral immature erythrocytes (MN%) and ratio of immature erythrocytes among total erythrocytes (IE%) are indicated. * and ** means $p < 0.05$, $p < 0.01$ in Mann–Whitney *U* test, respectively. Data represent mean ± S.D. ($n = 6$).

3.5. Recovery from MMC-induced DNA damage in the MEFs

To examine the role of Polk during recovery from DNA damage induced by MMC at the cellular level, we exposed MEFs from inactivated Polk KI and Polk⁺ mice to MMC *in vitro* and followed the kinetics of DNA damage with γH2AX as an index. The fluorescence intensity of γH2AX per nucleus reached the maximum levels 24 h after MMC treatment in MEFs of both inactivated Polk KI and Polk⁺ mice (Fig. 5). Interestingly, the fluorescence intensity remained constant for 120 h in MEFs of inactivated Polk KI mice while the fluorescence intensity disappeared gradually during the period in MEFs of Polk⁺ mice. On the other hand, apoptotic cells with condensed or fragmented nuclei were not observed even at the maximum dose in MEFs of either type of mice, therefore, the phosphorylation of H2AX was not thought to have been caused by apoptosis.

4. Discussion

MMC forms interstrand cross-links at CpG sites in opposite strands and intrastrand cross-links at GpG sites in the same strand of DNA [45]. Interstrand cross-links make two DNA strands inseparable, thereby inhibiting division of the strands and blocking DNA replication. There are two pathways to remove the lesion: S-phase-dependent and -independent interstrand cross-link repair [46,52]. In both pathways the cross-links are initially unhooked by endonucleases from one of the two DNA strands followed by TLS that bypasses the unhooked interstrand cross-link and restores one intact strand for homologous recombination [52]. Although Pol zeta and Rev1 are suggested to play roles in interstrand cross-link repair [53], it has been shown *in vitro* that Polk bypasses minor groove interstrand cross-links [29], that Polk plays a major role in S-phase-independent interstrand cross-link repair [54], and that cells deficient in Polk are sensitive to cytotoxicity of MMC [29]. Thus, we postulated that Polk plays substantial roles in repair of interstrand cross-links induced by MMC *in vivo*. In addition, regarding

Mice	Treatment	Number of bone marrow cells counted	Number of cells with γH2AX foci	Cells with foci (%)
Polk⁺	Saline	8820	4340	49
	MMC	8651	6491	75
Inactivated Polk KI	Saline	8744	4603	53
	MMC	8291	6622	80

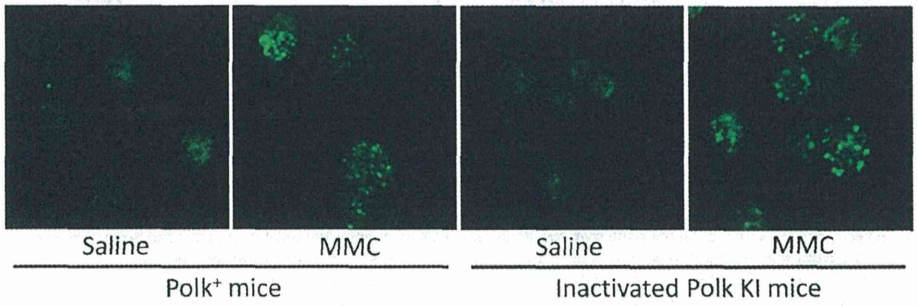

Fig. 4. Images of γH2AX foci in bone marrow cells and the number of cells with foci in each treatment group are shown. The cells were obtained 3 h after 5-day consecutive intraperitoneal injections of saline or MMC at 1 mg/kg/day from Polk⁺ and inactivated Polk KI mice. * and ** means $p < 0.05$ and $p < 0.01$ by Fisher's exact test, respectively.

the intrastrand cross-link, it is unclear which Pols are responsible for bypass beyond this type of cross-link.

To examine *in vivo* protective roles of Polk against the lesions induced by MMC, we generated inactivated Polk KI mice and analyzed mutations in the bone marrow. We hypothesized that, if Polk mediated error-free TLS over inter- and intrastrand cross-links, the frequency of mutations at CpG and GpG sequences would be enhanced. In fact, significant increase in MF of tandem base substitutions at GpG sites was observed in the inactivated Polk KI mice treated with MMC, while no significant increase was

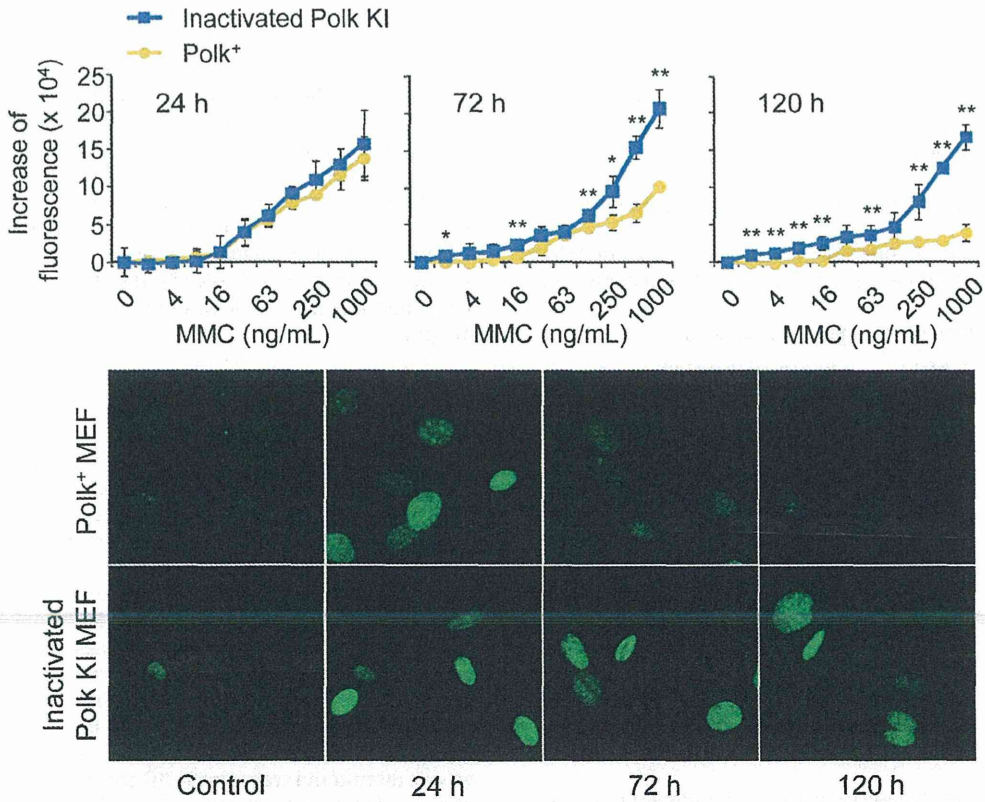

Fig. 5. Images of γH2AX fluorescence and average fluorescence intensity in the nucleus of MMC-treated MEFs. The MEFs were derived from Polk⁺ and inactivated Polk KI mice. Each MEF was treated with MMC at up to 1000 ng/mL for 24 h. The images were captured 24 h, 72 h, and, 120 h after treatment. One representative experiment of three is shown. Data represent mean ± S.D. ($n = 4$). * and ** means $p < 0.05$ and $p < 0.01$ by Student's *t*-test or Welch's test, respectively. The unit of fluorescence intensity is arbitrary.

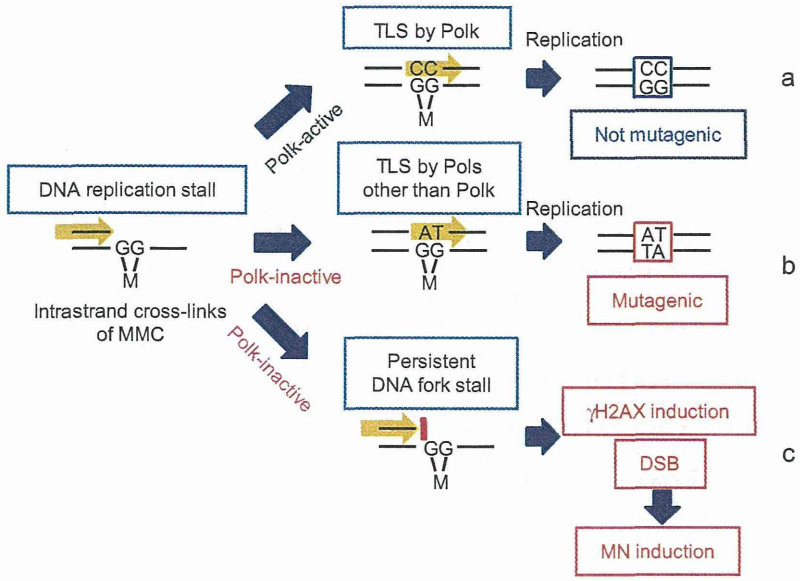

Fig. 6. A schematic of the roles of Polk in suppressing point mutations and DSBs caused by intrastrand cross-links by MMC. Replication by conventional Pols is blocked by MMC intrastrand cross-links. (a) When Polk is active, it is preferentially recruited at the site where DNA replication is blocked and conducts error-free TLS, which suppresses the induction of point mutations and DSBs in DNA. (b) When Polk is inactive, other Pols, such as Rev1 and Pol zeta, are recruited and conduct error-prone TLS, which results in effective suppression of DSBs with concomitant induction of point mutations. (c) Inactivation of Polk also increases the chances of DNA replication stall at the site of the lesion, which results in γH2AX formation and DSBs in DNA. Polk may play similar important protective roles against interstrand cross-links where an endonucleolytic incision makes unhooked lesions.

observed in Polk$^+$ mice (Fig. 2A, Table S1). In addition, the frequency of single- or tandem-base substitutions, insertions and short sequence substitutions at a CpG or GpG sequence or the flanking bases induced by MMC was significantly higher in inactivated Polk KI mice than in Polk$^+$ mice (Fig. 2B, Table 1, S2). MF of single-base deletions occurring at monotonic G or C sequences was also significantly increased by MMC treatment in inactivated Polk KI mice, but not in Polk$^+$ mice (Fig. 2B). Collectively, these results strongly suggest that Polk carries out error-free TLS beyond inter-strand and intrastrand cross-links induced by MMC in the bone marrow of mice (Fig. 6). When Polk is inactivated, other specialized Pols, such as Rev1 and Pol zeta, would be more frequently recruited to perform error-prone TLS across the cross-links, thereby inducing point mutations [39]. The enhancement of single-base deletions at monotonic G sequences after exposure to MMC was only observed in inactivated Polk KI mice (Fig. 2B, Table S2) in the present study and the enhancement did not occur in Polk wild phenotypes in previous studies [55,56]. We speculate, therefore, that Polk might be preferentially recruited to N^2–N^2 guanine intrastrand cross-links in guanine sequences to play a key role in suppressing frameshift mutations in the sequences.

In contrast to the point mutations described above, there was no difference in the MF of MMC-induced large deletions between inactivated Polk KI and Polk$^+$ mice (Table S3 and Fig. S5). Large deletion mutations detected by Spi$^-$ selection are generated by DSBs in DNA followed by error-prone repair, such as non-homologous end-joining [57]. Because Spi$^-$ selection may not detect deletions larger than 10 kbps [58], we compared the frequency of MNs in peripheral erythrocytes and the incidence of bone marrow cells with γH2AX foci in Polk$^+$ and inactivated Polk KI mice after MMC treatment to understand the contribution of Polk in suppressing DSBs in DNA. Interestingly, the MN frequency was significantly higher in inactivated Polk KI mice than Polk$^+$ mice (Fig. 3). The frequency of γH2AX-positive cells was also slightly but significantly higher in inactivated Polk KI mice than Polk$^+$ mice (Fig. 4). Therefore, we suggest that Polk plays a role in suppressing DSB induction by MMC (Fig. 6). Although Pol zeta and Rev1 may play major roles in suppression of large deletions [46,59,60], they induce point mutations because of their error-prone nature. Polk might complement the deficits of TLS mediated by these error-prone Pols by carrying out error-free TLS to suppress point mutations.

To examine the kinetics involved in recovery by Polk from DNA damage caused by cross-links, we measured γH2AX induction in MEFs derived from inactivated Polk KI and Polk$^+$ mice. Similar dose-dependent elevations of fluorescence intensity of γH2AX were observed in both MEFs at 24 h after the MMC treatment (Fig. 5). However, the γH2AX level at 120 h after treatment was much higher in the inactivated Polk KI MEF than in Polk$^+$ MEF. Phosphorylation of H2AX is mainly induced by DSBs in DNA, but is also induced by DNA replication stall or apoptosis [61,62]. In this study, no apoptotic morphologic changes were observed in MEFs even 120 h after the MMC treatment (Fig. 5). Hence, the delay in the γH2AX recovery in the inactivated Polk KI MEF may be attributed to persistent DNA replication blocks due to the lack of Polk activity, blocks which may result in DSBs in DNA (Fig. 6). We suggest that Polk contributes to the prevention of DSBs by resolving the replication blocks by carrying out TLS beyond inter- and intrastrand cross-links.

An increase in spontaneous mutations in Polk KO mice at 9 months and 12 months of age has been reported [34,35]. Base substitutions of G:C to T:A or G:C to C:G in liver and kidney, and G:C to A:T in lung are probably increased by intrinsic bulky DNA adducts. In our present study, an increase in spontaneous base substitutions of G:C to T:A was observed in inactivated Polk KI mice up to 14 weeks of age (Fig. 2A, Table S1), albeit this lacked statistical significance. However, elevated MF of G:C to C:G or G:C to A:T, as reported in Polk KO mice, was not detected while, on the other hand, the spontaneous −1G deletions observed in our inactivated Polk KI mice were not observed in the Polk KO mice. The discrepancy in mutation spectra might show that a lack of whole Polk protein, which includes an interactive domain with other Pols, in the KO mice affects recruitment of and interaction with other TLS Pols. Thus, the differences in mutation spectra might be attributed

to the difference of TLS Pols recruited in place of Polk. It would be interesting to see the difference in mutation spectra between inactivated Polk KI and KO mice after aging.

5. Conclusions

Although many *in vitro* studies have characterized the possible roles of Polk in repairing or preventing DNA damage, no convincing evidence for what roles Polk plays *in vivo* has been provided. We have established inactivated Polk KI mice with reporter genes for mutation analyses to examine the role of Polk in preventing DNA damage caused by MMC cross-links. The results indicate that Polk plays a predominant role in suppressing point mutations by carrying out error-free TLS across inter- and intrastrand cross-links *in vivo* (Fig. 6). The error-free TLS by Polk also contributes to the prevention of DSBs in DNA, although error-prone TLS mediated by other Pols, such as Pol zeta and Rev1, may play more major roles in the repair. The KI mice we have established will play a pivotal role in revealing the *in vivo* roles of Polk in repair and suppression of DNA lesions induced by a variety of endogenous and exogenous genotoxic stresses.

Conflict of interest

The authors declare no conflict of interest.

Acknowledgements

The authors thank Otoya Ueda for technical support; Yosuke Kawase and Toshio Hani for manipulation of mouse embryos; Takanori Tachibe, and Mami Kakefuda for breeding the transgenic mice; and Satomi Uchida, Yumiko Nakajima, Mariko Yano, Asako Harada, and, Kenji Tanaka for excellent technical assistance. The technical help of many contributors to this work is acknowledged. The authors thank Dr. Shuichi Chiba for critically reading the manuscript. This work was supported by grants in aid of scientific research from the Ministry of Education, Culture, Sports, Science and Technology, Japan (MEXT, 18201010; MEXT, 22241016), the Ministry of Health, Labour and Welfare, Japan (MHLW, H21-Food-General-009), and the Japan Health Science Foundation (KHB1007, KHB1006, KHB1209), and by grants in aid of cancer research from MHLW (20 designated-8) and the Food Safety Commission.

Appendix A. Supplementary data

Supplementary data associated with this article can be found, in the online version, at http://dx.doi.org/10.1016/j.dnarep.2014.09.002.

References

[1] E.C. Friedberg, et al., DNA Repair and Mutagenesis, second edition, ASM Press, Washington, DC, 2006, pp. 9–57.
[2] T.A. Kunkel, The high cost of living. American Association for Cancer Research Special Conference: endogenous sources of mutations, Fort Myers, Florida, USA, 11–15 November 1998, Trends Genet. 15 (3) (1999) 93–94.
[3] J.A. Swenberg, et al., Endogenous versus exogenous DNA adducts: their role in carcinogenesis, epidemiology, and risk assessment, Toxicol. Sci. 120 (Suppl 1:) (2011) S130–S145.
[4] E.C. Friedberg, R. Wagner, M. Radman, Specialized DNA polymerases, cellular survival, and the genesis of mutations, Science 296 (5573) (2002) 1627–1630.
[5] S. Prakash, R.E. Johnson, L. Prakash, Eukaryotic translesion synthesis DNA polymerases: specificity of structure and function, Annu. Rev. Biochem. 74 (2005) 317–353.
[6] T. Nohmi, Environmental stress and lesion-bypass DNA polymerases, Annu. Rev. Microbiol. 60 (2006) 231–253.
[7] S.D. McCulloch, T.A. Kunkel, The fidelity of DNA synthesis by eukaryotic replicative and translesion synthesis polymerases, Cell Res. 18 (1) (2008) 148–161.
[8] M.W. Schmitt, Y. Matsumoto, L.A. Loeb, High fidelity and lesion bypass capability of human DNA polymerase delta, Biochimie 91 (9) (2009) 1163–1172.
[9] S.S. Lange, K. Takata, R.D. Wood, DNA polymerases and cancer, Nat. Rev. Cancer 11 (2) (2011) 96–110.
[10] E.C. Friedberg, A.R. Lehmann, R.P. Fuchs, Trading places: how do DNA polymerases switch during translesion DNA synthesis? Mol. Cell 18 (5) (2005) 499–505.
[11] P.M. Burgers, et al., Eukaryotic DNA polymerases: proposal for a revised nomenclature, J. Biol. Chem. 276 (47) (2001) 43487–43490.
[12] J.E. Sale, A.R. Lehmann, R. Woodgate, Y-family DNA polymerases and their role in tolerance of cellular DNA damage, Nat. Rev. Mol. Cell Biol. 13 (3) (2012) 141–152.
[13] V.L. Gerlach, et al., Human DNA polymerase kappa: a novel DNA polymerase of unknown biological function encoded by the *DINB1* gene, Cold Spring Harb. Symp. Quant. Biol. 65 (2000) 41–49.
[14] T. Ogi, Y. Shinkai, K. Tanaka, H. Ohmori, Polk protects mammalian cells against the lethal and mutagenic effects of benzo[*a*]pyrene, Proc. Natl. Acad. Sci. U. S. A. 99 (24) (2002) 15548–15553.
[15] H. Ohmori, et al., The Y-family of DNA polymerases, Mol. Cell 8 (1) (2001) 7–8.
[16] J. Wagner, et al., The *dinB* gene encodes a novel *E. coli* DNA polymerase, DNA pol IV, involved in mutagenesis, Mol. Cell 4 (2) (1999) 281–286.
[17] P. Grúz, et al., Synthetic activity of *Sso* DNA polymerase Y1, an archaeal DinB-like DNA polymerase, is stimulated by processivity factors proliferating cell nuclear antigen and replication factor C, J. Biol. Chem. 276 (50) (2001) 47394–47401.
[18] A. Sassa, et al., Phenylalanine 171 is a molecular brake for translesion synthesis across benzo[*a*]pyrene-guanine adducts by human DNA polymerase kappa, Mutat. Res. 718 (1–2) (2011) 10–17.
[19] N. Suzuki, et al., Translesion synthesis by human DNA polymerase kappa on a DNA template containing a single stereoisomer of dG-(+)- or dG-(−)-*anti*-N^2-BPDE (7,8-dihydroxy-*anti*-9,10-epoxy-7,8,9,10-tetrahydrobenzo[*a*]pyrene), Biochemistry 41 (19) (2002) 6100–6106.
[20] N. Niimi, et al., The steric gate amino acid tyrosine 112 is required for efficient mismatched-primer extension by human DNA polymerase kappa, Biochemistry 48 (20) (2009) 4239–4246.
[21] A. Sassa, et al., In vivo evidence that phenylalanine 171 acts as a molecular brake for translesion DNA synthesis across benzo[*a*]pyrene DNA adducts by human DNA polymerase kappa, DNA Repair (Amst) 15 (2014) 21–28.
[22] J.Y. Choi, K.C. Angel, F.P. Guengerich, Translesion synthesis across bulky N^2-alkyl guanine DNA adducts by human DNA polymerase kappa, J. Biol. Chem. 281 (30) (2006) 21062–21072.
[23] X. Bi, D.M. Slater, H. Ohmori, C. Vaziri, DNA polymerase kappa is specifically required for recovery from the benzo[*a*]pyrene-dihydrodiol epoxide (BPDE)-induced S-phase checkpoint, J. Biol. Chem. 280 (23) (2005) 22343–22355.
[24] H. Fukuda, et al., Translesional DNA synthesis through a C8-guanyl adduct of 2-amino-1-methyl-6-phenylimidazo[4,5-*b*]pyridine (PhIP) in vitro: REV1 inserts dC opposite the lesion, and DNA polymerase kappa potentially catalyzes extension reaction from the 3′-dC terminus, J. Biol. Chem. 284 (38) (2009) 25585–25592.
[25] P.L. Fischhaber, et al., Human DNA polymerase kappa bypasses and extends beyond thymine glycols during translesion synthesis *in vitro*, preferentially *incorporating correct nucleotides*, J. Biol. Chem. 277 (40) (2002) 37604–37611.
[26] J.H. Yoon, G. Bhatia, S. Prakash, L. Prakash, Error-free replicative bypass of thymine glycol by the combined action of DNA polymerases kappa and zeta in human cells, Proc. Natl. Acad. Sci. U. S. A. 107 (32) (2010) 14116–14121.
[27] P. Jaloszyński, E. Ohashi, H. Ohmori, S. Nishimura, Error-prone and inefficient replication across 8-hydroxyguanine (8-oxoguanine) in human and mouse *ras* gene fragments by DNA polymerase kappa, Genes Cells 10 (6) (2005) 543–550.
[28] R. Vasquez-Del Carpio, et al., Structure of human DNA polymerase kappa inserting dATP opposite an 8-OxoG DNA lesion, PLoS One 4 (6) (2009) e5766.
[29] I.G. Minko, et al., Role for DNA polymerase kappa in the processing of N^2-N^2-guanine interstrand cross-links, J. Biol. Chem. 283 (25) (2008) 17075–17082.
[30] T. Ogi, A.R. Lehmann, The Y-family DNA polymerase kappa (pol kappa) functions in mammalian nucleotide-excision repair, Nat. Cell Biol. 8 (6) (2006) 640–642.
[31] R. Bétous, et al., DNA polymerase kappa-dependent DNA synthesis at stalled replication forks is important for CHK1 activation, EMBO J. 32 (15) (2013) 2172–2185.
[32] X. Zhang, et al., Mouse DNA polymerase kappa has a functional role in the repair of DNA strand breaks, DNA Repair (Amst) 12 (5) (2013) 377–388.
[33] B.A. Baptiste, K.A. Eckert, DNA polymerase kappa microsatellite synthesis: two distinct mechanisms of slippage-mediated errors, Environ. Mol. Mutagen. 53 (9) (2012) 787–796.
[34] J.N. Stancel, et al., *Polk* mutant mice have a spontaneous mutator phenotype, DNA Repair (Amst) 8 (12) (2009) 1355–1362.
[35] W.D. Singer, L.C. Osimiri, E.C. Friedberg, Increased dietary cholesterol promotes enhanced mutagenesis in DNA polymerase kappa-deficient mice, DNA Repair (Amst) 12 (10) (2013) 817–823.
[36] E. Ohashi, et al., Interaction of hREV1 with three human Y-family DNA polymerases, Genes Cells 9 (6) (2004) 523–531.
[37] E. Ohashi, et al., Identification of a novel REV1-interacting motif necessary for DNA polymerase kappa function, Genes Cells 14 (2) (2009) 101–111.
[38] X. Bi, et al., Rad18 regulates DNA polymerase kappa and is required for recovery from S-phase checkpoint-mediated arrest, Mol. Cell Biol. 26 (9) (2006) 3527–3540.
[39] J. Wojtaszek, et al., Structural basis of Rev1-mediated assembly of a quaternary vertebrate translesion polymerase complex consisting of Rev1, heterodimeric polymerase (Pol) zeta, and Pol kappa, J. Biol. Chem. 287 (40) (2012) 33836–33846.

[40] H.D. Ulrich, T. Takahashi, Readers of PCNA modifications, Chromosoma 122 (4) (2013) 259–274.
[41] T. Nohmi, et al., A new transgenic mouse mutagenesis test system using Spi⁻ and 6-thioguanine selections, Environ. Mol. Mutagen. 28 (4) (1996) 465–470.
[42] T. Nohmi, T. Suzuki, K. Masumura, Recent advances in the protocols of transgenic mouse mutation assays, Mutat. Res. 455 (1–2) (2000) 191–215.
[43] T. Nohmi, Novel DNA polymerases and novel genotoxicity assays, Genes Environ. 29 (3) (2007) 75–88.
[44] T. Nohmi, K. Masumura, Molecular nature of intrachromosomal deletions and base substitutions induced by environmental mutagens, Environ. Mol. Mutagen. 45 (2–3) (2005) 150–161.
[45] M. Tomasz, A.K. Chawla, R. Lipman, Mechanism of monofunctional and bifunctional alkylation of DNA by mitomycin C, Biochemistry 27 (9) (1988) 3182–3187.
[46] T.V. Ho, O.D. Schärer, Translesion DNA synthesis polymerases in DNA interstrand crosslink repair, Environ. Mol. Mutagen. 51 (6) (2010) 552–566.
[47] A.J. Deans, S.C. West, DNA interstrand crosslink repair and cancer, Nat. Rev. Cancer 11 (7) (2011) 467–480.
[48] T. Tominaga, et al., Activation of bone morphogenetic protein 4 signaling leads to glomerulosclerosis that mimics diabetic nephropathy, J. Biol. Chem. 286 (22) (2011) 20109–20116.
[49] G.J. Carr, N.J. Gorelick, Mutational spectra in transgenic animal research: data analysis and study design based upon the mutant or mutation frequency, Environ. Mol. Mutagen. 28 (4) (1996) 405–413.
[50] C. Guo, et al., Multiple *PolK (POLK)* transcripts in mammalian testis, DNA Repair (Amst) 4 (3) (2005) 397–402.
[51] T. Nohmi, et al., Spi⁻ selection: An efficient method to detect gamma-ray-induced deletions in transgenic mice, Environ. Mol. Mutagen. 34 (1) (1999) 9–15.
[52] G.L. Moldovan, A.D. D'Andrea, How the fanconi anemia pathway guards the genome, Annu. Rev. Genet. 43 (2009) 223–249.
[53] S. Sharma, C.E. Canman, REV1 and DNA polymerase zeta in DNA interstrand crosslink repair, Environ. Mol. Mutagen. 53 (9) (2012) 725–740.
[54] H.L. Williams, M.E. Gottesman, J. Gautier, Replication-independent repair of DNA interstrand crosslinks, Mol. Cell 47 (1) (2012) 140–147.
[55] A. Takeiri, et al., Molecular characterization of mitomycin C-induced large deletions and tandem-base substitutions in the bone marrow of *gpt* delta transgenic mice, Chem. Res. Toxicol. 16 (2) (2003) 171–179.
[56] A. Takeiri, et al., A newly established GDL1 cell line from *gpt* delta mice well reflects the *in vivo* mutation spectra induced by mitomycin C, Mutat. Res. 609 (1) (2006) 102–115.
[57] M. Horiguchi, et al., Molecular nature of ultraviolet B light-induced deletions in the murine epidermis, Cancer Res. 61 (10) (2001) 3913–3918.
[58] T. Nohmi, K. Masumura, *gpt* delta transgenic mouse: a novel approach for molecular dissection of deletion mutations *in vivo*, Adv. Biophys. 38 (2004) 97–121.
[59] S. Shachar, et al., Two-polymerase mechanisms dictate error-free and error-prone translesion DNA synthesis in mammals, EMBO J. 28 (4) (2009) 383–393.
[60] J.M. Brondello, et al., Novel evidences for a tumor suppressor role of Rev3, the catalytic subunit of Pol zeta, Oncogene 27 (47) (2008) 6093–6101.
[61] W.M. Bonner, et al., GammaH2AX and cancer, Nat. Rev. Cancer 8 (12) (2008) 957–967.
[62] J.E. Cleaver, L. Feeney, I. Revet, Phosphorylated H2Ax is not an unambiguous marker for DNA double-strand breaks, Cell Cycle 10 (19) (2011) 3223–3224.

Biochemical Pharmacology 89 (2014) 340–348

Contents lists available at ScienceDirect

Biochemical Pharmacology

journal homepage: www.elsevier.com/locate/biochempharm

DIF-1 inhibits tumor growth *in vivo* reducing phosphorylation of GSK-3β and expressions of cyclin D1 and TCF7L2 in cancer model mice

Fumi Takahashi-Yanaga [a,b,*], Tatsuya Yoshihara [a], Kentaro Jingushi [a], Kazuhiro Igawa [c], Katsuhiko Tomooka [c], Yutaka Watanabe [d], Sachio Morimoto [a], Yoshimichi Nakatsu [e], Teruhisa Tsuzuki [e], Yusaku Nakabeppu [f], Toshiyuki Sasaguri [a,*]

[a] Department of Clinical Pharmacology, Faculty of Medical Sciences, Kyushu University, Fukuoka, Japan
[b] Global Medical Science Education Unit, Faculty of Medical Sciences, Kyushu University, 3-1-1 Maidashi, Higashi-ku, Fukuoka 812-8582, Japan
[c] Department of Molecular and Material Science, Institute for Materials Chemistry and Engineering, Kyushu University, Fukuoka, Japan
[d] Department of Applied Chemistry, Faculty of Engineering, Ehime University, Matsuyama, Japan
[e] Department of Medical Biophysics and Radiation Biology, Faculty of Medical Sciences, Kyushu University, Fukuoka, Japan
[f] Division of Neurofunctional Genomics, Department of Immunobiology and Neuroscience, Medical Institute of Bioregulation, Kyushu University, Fukuoka, Japan

ARTICLE INFO

Article history:
Received 10 February 2014
Received in revised form 12 March 2014
Accepted 14 March 2014
Available online 23 March 2014

Keywords:
DIF-1
TCF7L2
GSK-3β
Wnt/β-catenin signaling pathway
Egr-1

ABSTRACT

We reported that differentiation-inducing factor-1 (DIF-1), synthesized by *Dictyostelium discoideum*, inhibited proliferation of various tumor cell lines *in vitro* by suppressing the Wnt/β-catenin signaling pathway. However, it remained unexplored whether DIF-1 also inhibits tumor growth *in vivo*. In the present study, therefore, we examined *in-vivo* effects of DIF-1 using three cancer models: *Mutyh*-deficient mice with oxidative stress-induced intestinal tumors and nude mice xenografted with the human colon cancer cell line HCT-116 and cervical cancer cell line HeLa. In exploration for an appropriate route of administration, we found that orally administered DIF-1 was absorbed through the digestive tract to elevate its blood concentration to levels enough to suppress tumor cell proliferation. Repeated oral administration of DIF-1 markedly reduced the number and size of intestinal tumors that developed in *Mutyh*-deficient mice, reducing the phosphorylation level of GSK-3β Ser^9 and the expression levels of early growth response-1 (Egr-1), transcription factor 7-like 2 (TCF7L2) and cyclin D1. DIF-1 also inhibited the growth of HCT-116- and HeLa-xenograft tumors together with decreasing phosphorylation level of GSK-3β Ser^9, although it was not statistically significant in HeLa-xenograft tumors. DIF-1 also suppressed the expressions of Egr-1, TCF7L2 and cyclin D1 in HCT-116-xenograft tumors and those of β-catenin, TCF7L2 and cyclin D1 in HeLa-xenograft tumors. This is the first report to show that DIF-1 inhibits tumor growth *in vivo*, consistent with its *in-vitro* action, suggesting that this compound may have potential as a novel anti-tumor agent.

1. Introduction

The Wnt/β-catenin signaling pathway, which is well conserved throughout biological evolution, regulates a number of cellular functions during embryonic development and in maintenance of tissue homeostasis by regulating somatic stem cells and their niches [1–3]. Accumulating evidence suggests that this pathway is often involved in oncogenesis and cancer development. Activation of the Wnt/β-catenin signaling pathway results in upregulation of its target genes, such as *CCND1* encoding cyclin D1 and *c-myc*, which play key roles in the initiation and progression of G_1 phase in the cell cycle [4,5], thereby promoting tumor formation [6–9]. In fact, this pathway is constitutively activated in most colorectal cancers, including those in patients with familial adenomatous polyposis (FAP), and other types of malignant tumors [10–14].

Glycogen synthase kinase-3β (GSK-3β) was first identified as a cytoplasmic serine/threonine protein kinase that phosphorylates glycogen synthase to inhibit its activity. However, it is now well known that this kinase plays central roles in various biological

* Corresponding authors at: Department of Clinical Pharmacology, Faculty of Medical Sciences, Kyushu University, 3-1-1 Maidashi, Higashi-ku, Fukuoka 812-8582, Japan. Tel.: +81 92 642 6887; fax: +81 92 642 6084.
E-mail addresses: yanaga@cliphrarm.med.kyushu-u.ac.jp (F. Takahashi-Yanaga), sasaguri@cliphrarm.med.kyushu-u.ac.jp (T. Sasaguri).

http://dx.doi.org/10.1016/j.bcp.2014.03.006
0006-2952/